

# Processing and Microstructure of Investment Casting Turbine Blade NITAC In-Situ Composites

*E. Fras, E. Guzik, W. Kapturkiewicz, and H.F. López*

Directional solidification was used to produce turbine blades by the Bridgman method. NITAC alloys with various carbon contents were investigated; the optimum range was found to be 0.40 to 0.48%. Within this range, except for the blade locking piece edges, the blade structure consisted predominantly of aligned eutectics. The in-situ eutectics were aligned tantalum fibers embedded in a  $\gamma$ -phase matrix. The blades were produced using an alloy displacement rate of  $1.86 \times 10^{-6}$  m/s. Measurements of fiber spacings along the blade height indicated that the rate of displacement of the solidification front exhibited some variations. These variations were closely associated with dimensional changes in the turbine blade cross sections.

## Keywords

directionally solidified superalloys, in-situ eutectics, NITAC alloys, single-crystal turbine blades

## 1. Introduction

BECAUSE turbine blades play a key role in the performance of advanced turbine engines, a number of critical conditions must be satisfied in order to ensure adequate operation at working temperatures (Ref 1). These conditions include high-temperature creep strength and thermal and mechanical fatigue strength. Since the efficiency of turbine engines increases with temperature, considerable effort has been directed toward the development of advanced alloys for stable operation under extreme conditions (i.e., temperatures above 1000 °C).

Early attempts were based on the use of single  $\gamma$ -phase nickel-base superalloys. These alloys performed satisfactorily at temperatures as high as 830 °C. Later on, other alloy compositions were developed to incorporate the effect of ordered  $\gamma'$  precipitates that form inside the  $\gamma$ -phase matrix. These phases promoted alloy strengthening by effectively blocking dislocation climb, but severely impaired alloy forgeability. Consequently, blades made from these alloys were produced using investment casting techniques and vacuum metallurgy. By these means, turbine blade operating temperatures were increased up to 940 °C. At elevated temperatures, grain boundaries may become preferred sites for intergranular cavitation and fissuring. This posed difficulties in terms of achieving even higher blade operating temperatures. The grain-boundary effect was minimized or avoided through the development of blades made of either aligned or single crystals (second-generation blades) that can be used at temperatures up to 970 or 1000 °C, respectively.

**E. Fras**, University of Mines and Metallurgy, Reymonta 23, Cracow, Poland (presently at Centro de Investigación y Asistencia técnica del Estado de Queretaro [CIATEQ], Calzada del Retablo No. 150, 76150 Qro. México); **E. Guzik** and **W. Kapturkiewicz**, University of Mines and Metallurgy, Reymonta 23, Cracow, Poland; and **H.F. López**, Materials Department, University of Wisconsin-Milwaukee, Milwaukee, WI, 53201, USA.

In order to further increase blade operating temperatures, alloy reinforcements based on continuous aligned fibers have been considered (Ref 2). Unfortunately, blade production using composite materials is rather limited due to the high costs involved. Unidirectional solidification can be considered as a viable alternative in the development of fiber-reinforced turbine blades for alloys of eutectic composition. In unidirectional solidification, a planar front unfolds where one or more eutectic phases nucleate and grow as aligned fibers. The resultant structure is made of narrowly spaced eutectic fibers, producing superior mechanical strength. For example, the strength of a conventionally solidified Fe-29Cr-2.9C-0.005Ti alloy improves dramatically when the alloy is solidified unidirectionally; tensile strength increases from 700 to 3100 MPa (Ref 3). Figure 1 shows schematically the various grain structures used in turbine blade production.

Recent trends in alloy development have led to the consideration of Ni-Ta-C (NITAC) or Co-Ta-C (COTAC) alloys (Ref 4-6) for turbine blade applications. Figure 2 compares the strength exhibited by NITAC, COTAC, and MAR 200-GE alloys as a function of the Larson-Miller parameter. Figure 3 shows chronologically how the incorporation of in-situ eutectics in turbine blades has led to the highest operating temperatures. Accordingly, blades made of in-situ composite eutectics can be considered as a third generation in turbine blade development. These types of blades are expected to increase working temperatures by approximately 60 °C and to reduce fuel consumption by approximately 10%.

Although the technology necessary for the production of eutectic composite blades is already available, no information can be found in the literature on alloy chemistry, temperature gradients, growth rates, or the microstructures and macrostructures that result from unidirectional solidification. This lack of information is probably due to the inherent complications associated with obtaining ideal in-situ microstructures for as-cast turbine blades (see Fig. 1d and e). Thus far, knowledge of the effect of casting shape on the expected microstructure is rather limited. This is particularly important when considering thick and thin cast sections (such as links between blade leaf and locking piece). Hence, the present work aimed to determine optimum processing parameters and resultant microstructures for

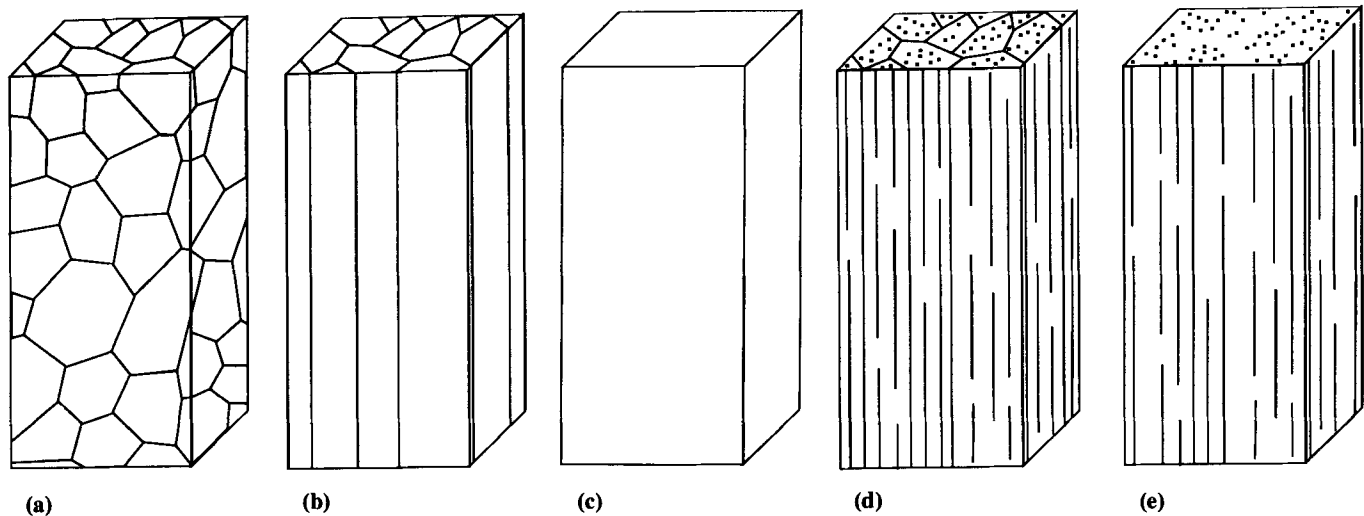


**Fig. 1** Schematic representation of grain structure in turbine blades. (a) First-generation blades consisting of equiaxed grains. (b) Second-generation blades with columnar grains. (c) Second-generation blades with monocrystals. (d) Third-generation blades with columnar grains. (e) Third-generation blades with monocrystals. Structures (d) and (e) are reinforced with high-strength fibers.

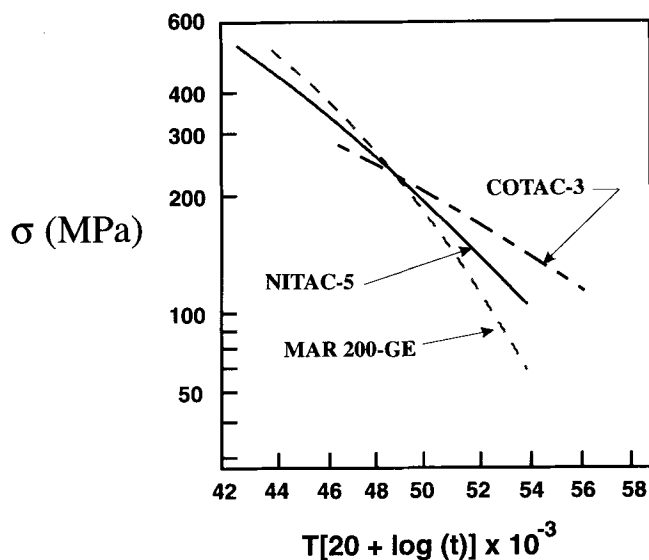


**Fig. 2** Larson-Miller parameter curves for in-situ high-temperature eutectic alloys. Source: Ref 7

turbine blades produced by unidirectional solidification of NITAC eutectic alloys (in-situ composites).

## 2. Materials and Methods

### 2.1 Alloy Preparation

The investigated NITAC alloy was produced in a Balzers vacuum furnace (VSG.02) using high-purity (99.99%) chromium, cobalt, aluminum, and tantalum, as well as electrolytic nickel (99.7% pure). Carbon was introduced as spectrographic pure graphite. The metal bath was isothermally kept at 1650 °C under 13.3 MPa until complete bath deoxidation occurred. This was followed by melt pouring into cylindrical ceramic molds.

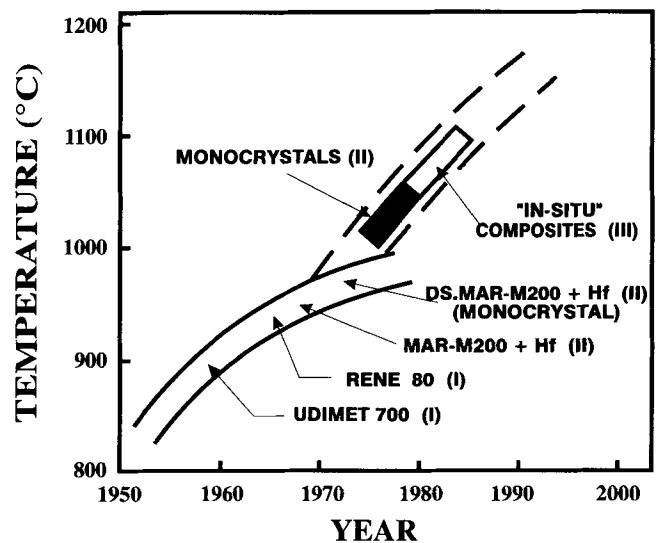


**Fig. 3** Chronological evolution of high-operating-temperature turbine blade alloys. I, II, and III are successive generations.

Ingot rods of 22 mm diameter were produced and cut into approximately 80 g bars, which were then used as the base alloy for unidirectional solidification. The amount of carbon introduced in the bath was systematically varied between 0.29 and 0.60%. The resultant alloy composition was Ni-20Co-10.85Ta-10Cr-3A.

### 2.2 Mold Preparation

Turbine blade ceramic molds closely reproduced the blade shape, accounting for material tolerances. The ceramic shell closely adhered to the wax model. The blade cast models, including raisers and starters, were made from imported British Wax mixture A74101. The raiser head was used to introduce the alloy, which upon melting filled the mold cavity; the starter was

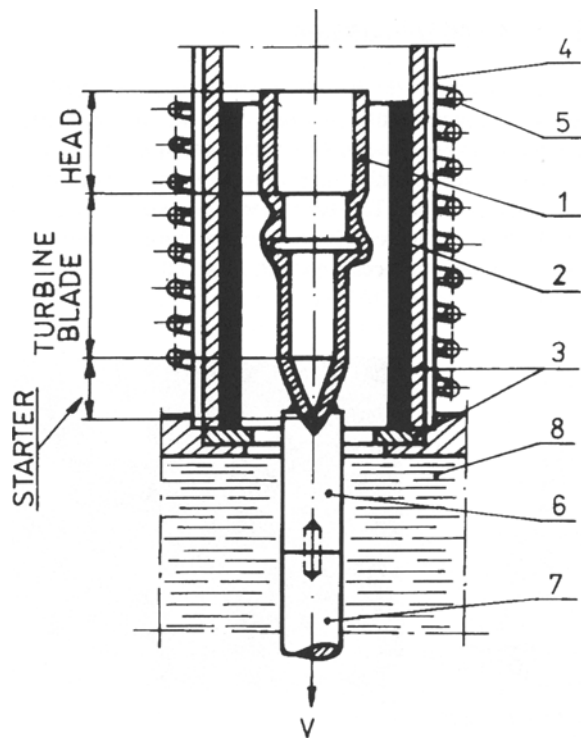


**Fig. 4** Schematic diagram of unidirectional solidification apparatus: 1, ceramic mold; 2, graphite tube; 3, insulation; 4, quartz tube; 5, coil; 6, graphite stool; 7, pulling rod; 8, liquid tin

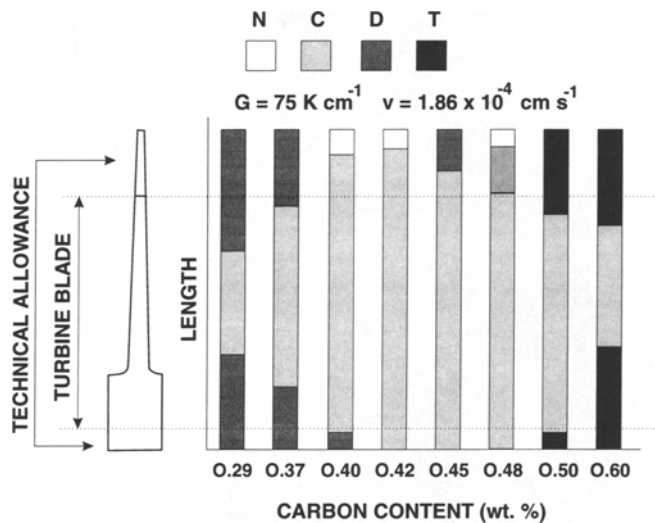
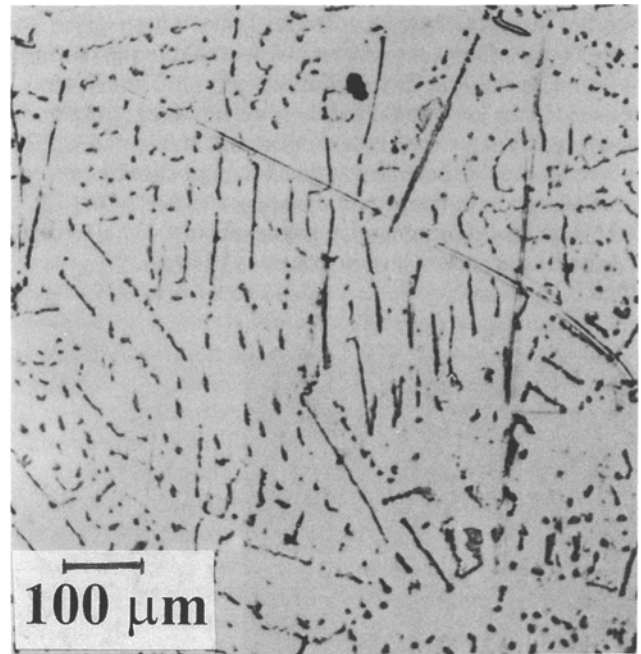
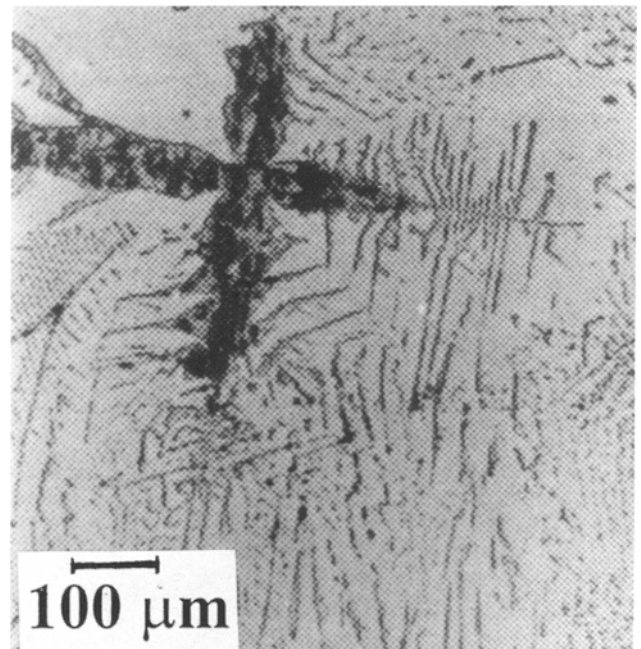


**Fig. 5** Effect of carbon content in the NITAC alloy on the type and extent of structural zones in a turbine blade

used for preorientation of the resultant alloy structure during unidirectional solidification. Wax models were immersed in a liquid mixture containing stabilized zirconia and colloidal silica as a binding agent. After drying, the first layer of ceramic shell was obtained. Four successive ceramic shells were then applied using colloidal silica and hydrated ethyl silicate as binder and aloxite as refractory material. Wetting and antirubbing substances also were introduced in the ceramic mixtures.



(a)



(b)

**Fig. 6** Directionally solidified N-type (a) and T-type (b) microstructures. Unetched to avoid disclosing the  $\gamma'$ -phase.

Once these forms dried in an oven, they were used to cast a wax model and then heated at 1000 °C for 8 h.

### 2.3 Solidification

Directional solidification of turbine blade NITAC alloys was carried out in a Bridgman apparatus (liquid-cooling

method). Construction design details of this unit are given in Ref 8. Figure 4 shows the location of the mold in the heating chamber of the unidirectional solidification unit. The alloy was introduced in the blade mold and then melted under pure argon until the bath temperature was stabilized at 1650 to 1670 °C. Unidirectional solidification was then accomplished by pulling the mold through the temperature gradient at either  $1.86 \times 10^{-6}$  or  $3.72 \times 10^{-6}$  m/s. The temperature gradient in the liquid metal just preceding the solidification front was 75 K/cm.

### 3. Results and Discussion

According to eutectic solidification models (Ref 9,10), coupled growth of two eutectic phases from a liquid of noneutectic composition can generate in-situ composite structures. For this to occur, a flat stable solidification front must be developed at the macroscopic level. The type of solidification front generated is strongly influenced by the temperature gradient in the liquid,  $G$ ; the rate of eutectic growth,  $v$ ; and the alloy composition.

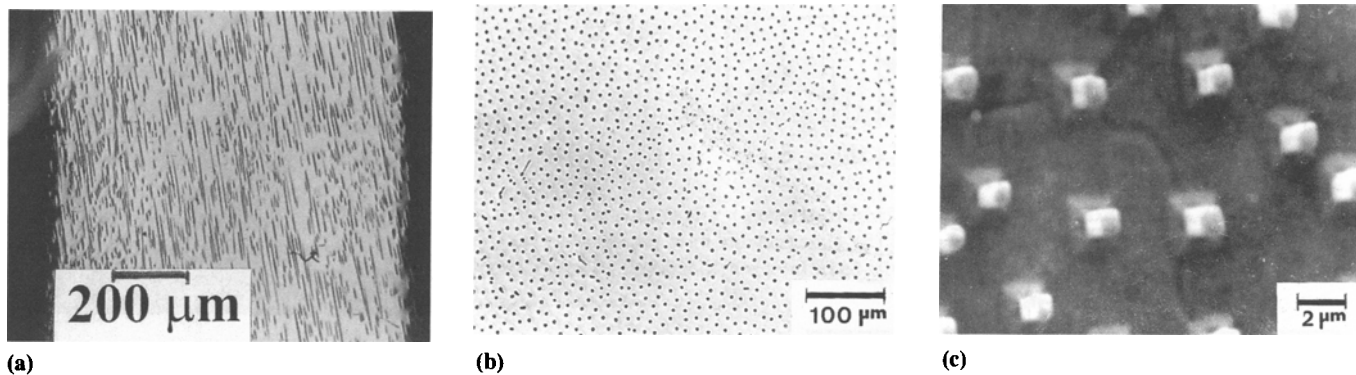


**Fig. 7** Longitudinal section (a) and cross section (b) of C-type microstructures. (c) Higher-magnification view of cross section

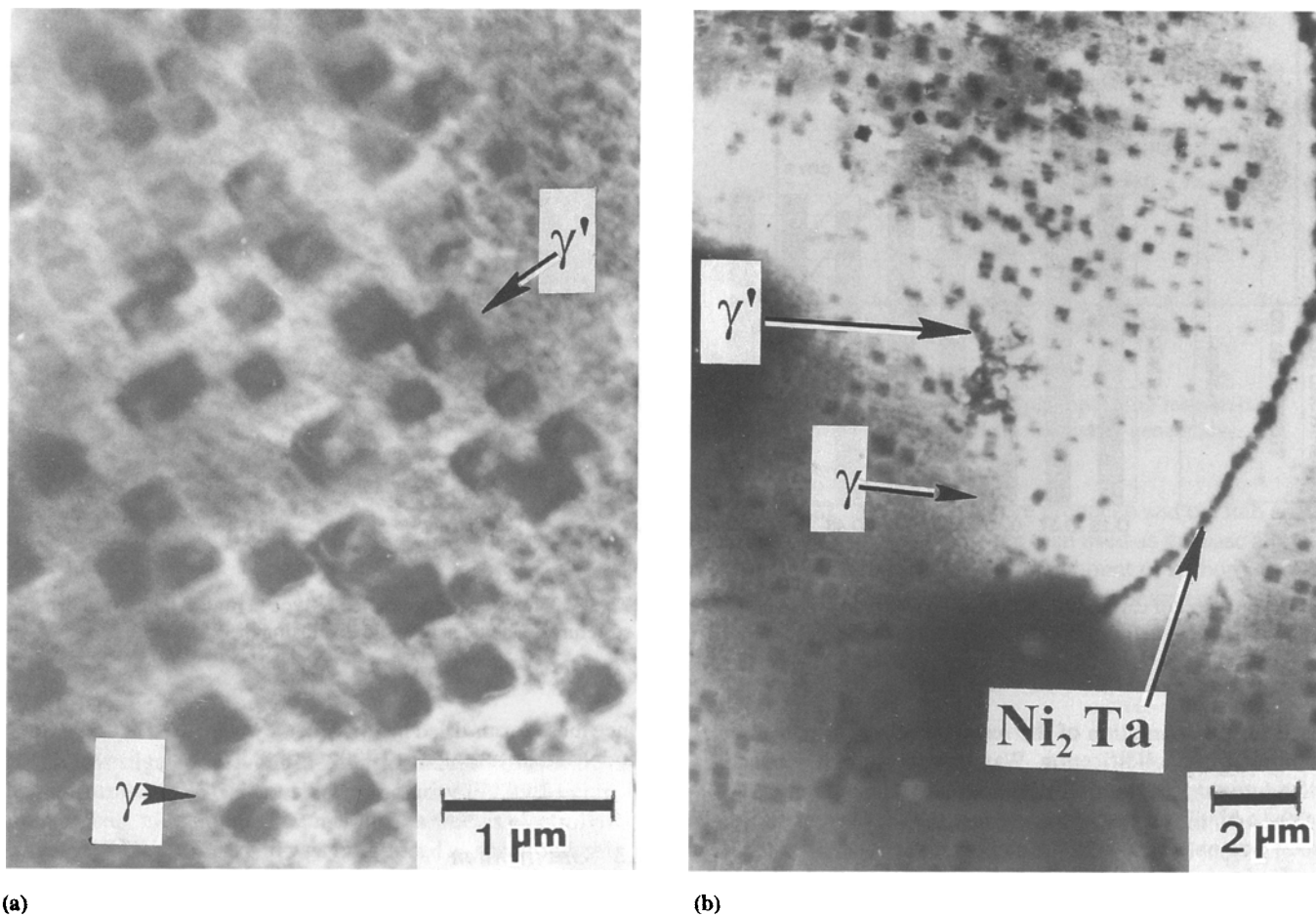


**Fig. 8** (a) Matrix structure. (b) Lower-magnification view

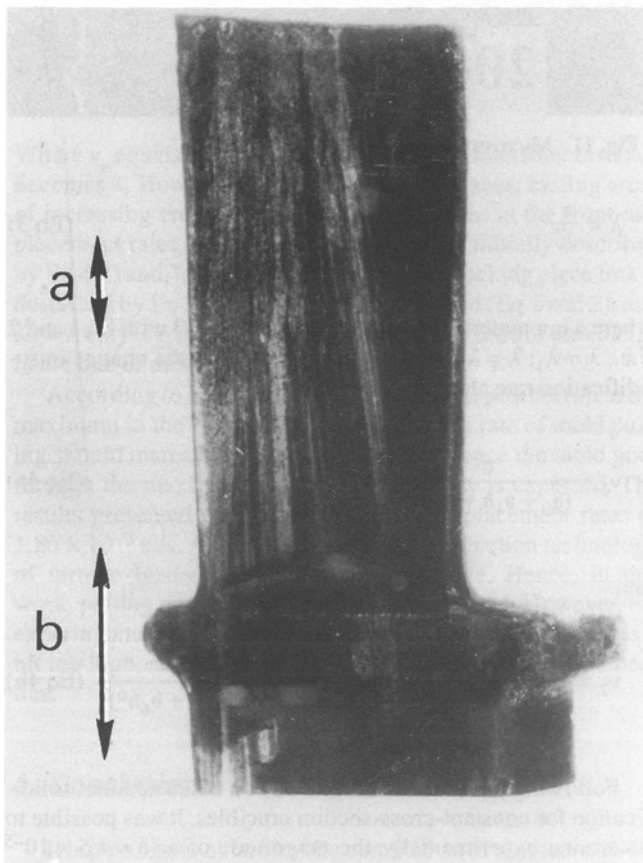
tion, *DC*. Zones of coupled eutectic growth are known for a number of binary alloys (*G/v-DC* maps of regions where coupled growth of eutectic phases occurs). This enables the selection of composition and alloy conditions that give rise to desired eutectics (in-situ composites), excluding any proeutectic phases. In multicomponent alloys such as NITAC, the coupled zone region for eutectic growth is not yet known. Hence, in order to obtain a flat solidification front for a given *G/v* ratio (typical of the solidification apparatus), it was necessary to vary the carbon content of the NITAC alloy. Various carbon concentrations were considered until an optimum range (0.42 to 0.46% C) was established.

Turbine blades with in-situ eutectic structures were metallographically examined. A number of cuts were made in the longitudinal and transverse blade orientation in order to determine the morphological variations effected by the blade shape. The type and extent of a particular microstructural zone were correlated with carbon content, as shown in Fig. 5. Three principal microstructures were obtained at growth rates of  $1.86 \times 10^{-6}$  m/s (zones N, T, and C in Fig. 6 and 7). The N-type structure (Fig. 6a) included nonaligned eutectics (TaC + matrix), whereas the T-type structure (Fig. 6b) consisted of large proeutectic TaC precipitates as well as eutectic. Figure 7 shows longitudinal and transverse sections of oriented eutectic composites (C-type structures). In addition,  $\gamma' \text{Ni}_3(\text{Ta,Al})$  cubic precipitates (Fig. 8a) were found in the  $\gamma$ -phase matrix, along with precipitation of  $\text{Ni}_2\text{Ta}$  particles along grain inter-

faces (see arrow in Fig. 8b). Both precipitates are expected to further enhance the matrix strength of the in-situ composite.

As shown in Fig. 5, the alloy with the lowest carbon content (0.29% C) exhibits only a relatively small region for the development of in-situ composites (zone C). As the carbon content increases, this region continues to expand and reaches a maximum at 0.42% C. Hence, with the exception of the blade locking edges, in-situ eutectic structures for turbine blades can be obtained for carbon contents of 0.40 to 0.48%. The macrostructure of a turbine blade made of an alloy containing 0.45% C (without the starter) is shown in Fig. 9(a). Notice that unidirectional solidification has a radical effect on the macrostructure of the casting, producing columnar grains that generally lie parallel to the alloy displacement orientation within the furnace. Conventional solidification, on the other hand, gives rise to small equiaxed grains (Fig. 9b).

For all the carbon contents investigated, it was impossible to remove the microstructural defects from the locking piece edges (Fig. 10). These edges were made up of eutectic grains with nonaligned fibers or of  $\gamma$ -phase dendrites. Furthermore, the angle between two eutectic grains (arrows in Fig. 10) seems to extend from the blade leaf to the locking piece as a "wedge" but does not weaken this region. Accordingly, the blade locking piece might not consist of fully aligned eutectics in unidirectionally solidified blades as suggested by Thompson (Ref 11). The microstructure of the longitudinal section (zone b, Fig. 9a) of a blade leaf is shown in Fig. 11. Notice that the TaC fibers are



(a)



(b)

**Fig. 9** Turbine blade macrostructures obtained by unidirectional solidification (a), and by conventional methods (b)

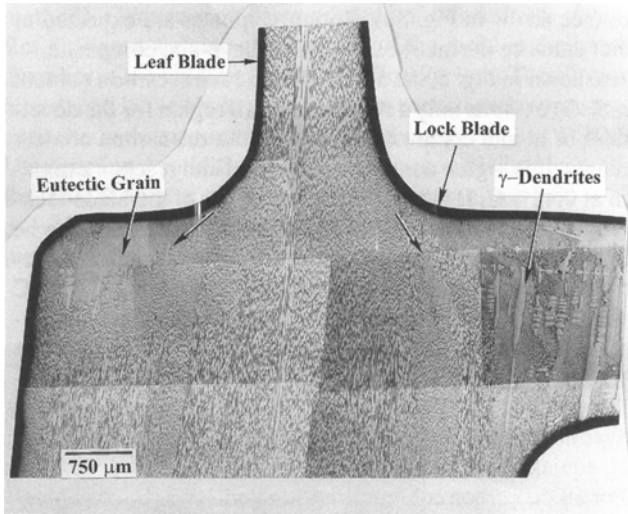


**Fig. 10** Microstructure of a turbine blade section from the region of the locking piece corresponding to zone b in Fig. 9(a). Unetched

not ideally parallel to the blade major axis, but exhibit an angular deviation of  $2^\circ$  with respect to the mold contour. This angular variation can be considered a minor microstructural fault produced during solidification.

The development of angular deviations in the fiber orientation of the blade leaf results from the relative location of the induction coil with respect to the solidification front. The induction coil generates isotherms that are parallel to this front. Hence, fibers grow normal to the developed isotherms. Proper alignment of the induction coil should eliminate the development of angular deviations in the fiber orientation. In practice, however, geometrical constraints make it difficult to accurately align the induction coil so that all of the main blade axes remain normal to the solidification front.

Measurements of interfiber spacings ( $\lambda$ ) made from cross sections of the blade leaf and locking piece are shown in Fig. 12. It is apparent that  $\lambda$  remains almost constant until reaching the blade leaf/locking piece link, where it undergoes a significant shift. Variations in the  $\lambda$  values indicate a change in the displacement rate of the solidification front. Hence, it can be assumed that solidification of the turbine blade occurs under unstable growth conditions induced by the cross-sectional variations of the turbine blade (leaf/locking piece). Statistically, the curve shown in Fig. 12 can be described by:

$$\lambda_1 = a_0 + a_1h + a_2h^2 \quad (\text{Eq 1})$$

and

$$\lambda_2 = b_0 + b_1h + b_2h^2 + b_3h^3 + b_4h^4 + b_5h^5 + b_6h^6 \quad (\text{Eq 2})$$

where  $h$  is blade height, and  $a_i$  and  $b_i$  are statistically determined constants. Assuming the following relationship between solidification rate ( $v$ ) and  $\lambda$ :

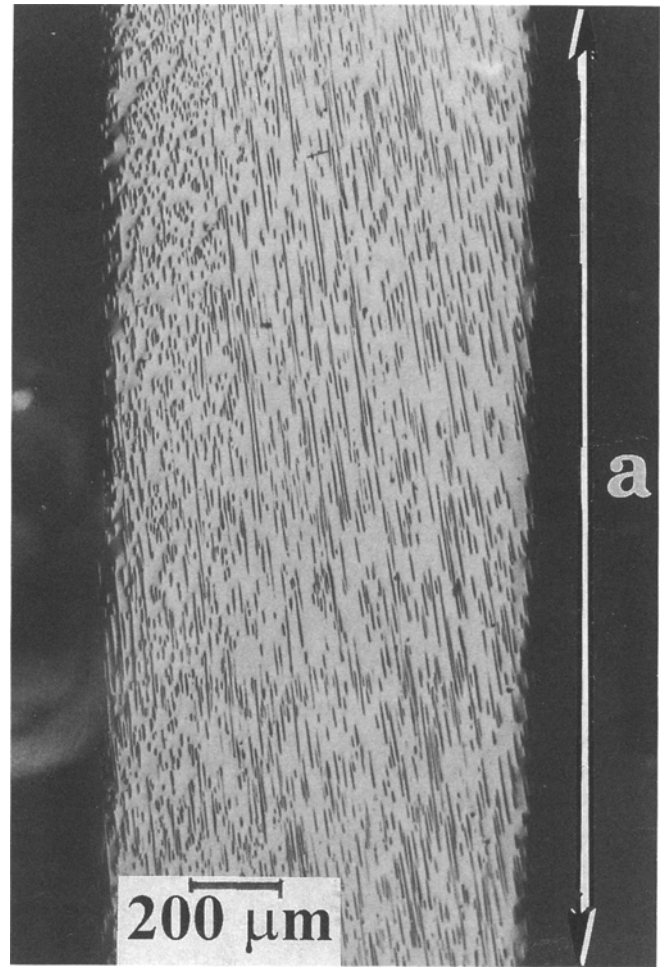


**Fig. 11** Microstructure of leaf blade. Unetched

$$\lambda = \frac{a}{\sqrt{v}} \quad (\text{Eq 3})$$

where  $a$  is a material constant. Comparing Eq 3 with Eq 1 and 2 (i.e.,  $\lambda = \lambda_1$ ;  $\lambda = \lambda_2$ ) yields an expression for the change in solidification rate along the blade height:

$$v_1 = \frac{a^2}{(a_0 + a_1h + a_2h^2)^2} \quad (\text{Eq 4a})$$

and

$$v_2 = \frac{a^2}{(b_0 + b_1h + b_2h^2 + b_3h^3 + b_4h^4 + b_5h^5 + b_6h^6)^2} \quad (\text{Eq 4b})$$

Following previous work (Ref 12) on unidirectional solidification for constant-cross-section crucibles, it was possible to determine experimentally the magnitude of  $a$  ( $a = 4.5 \times 10^{-5} \text{ cm}^{3/2}/\text{s}^{1/2}$ ) for the NITAC alloy. Hence, in order to obtain a constant  $\lambda$  along the entire blade length, the growth rate  $v$  (Eq 4 and 5) must be controlled. Assuming that during solidification of

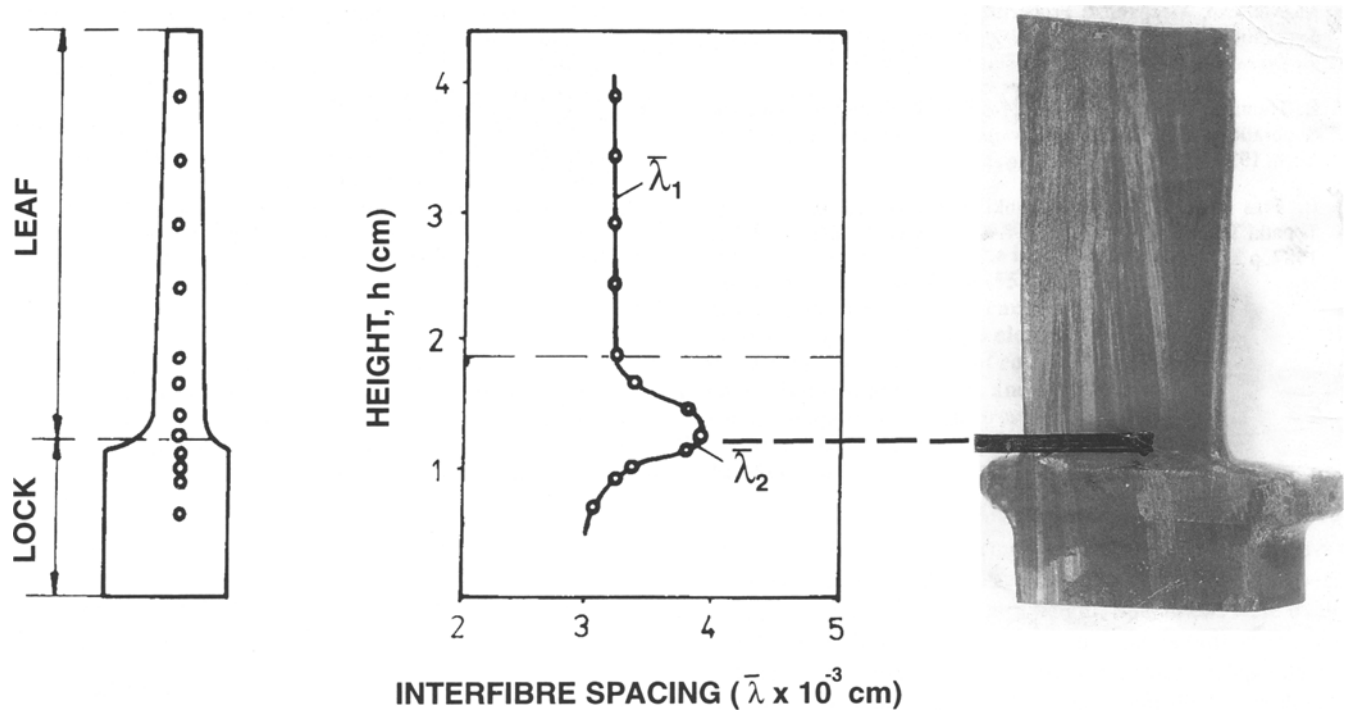


Fig. 12 (Right) Longitudinal section of turbine blade. (Left) A-A cut (schematic). (Center) Interfiber spacing as a function of blade height

the blade leaf, the displacement rate at the solidification front is given by:

$$v_p = (a/\lambda)^2 \quad (\text{Eq 5})$$

Where  $v_p$  equals the rate of mold pulling, the interfiber distance becomes  $\lambda$ . However, as solidification continues, casting areas of increasing cross section lead to reductions in the front displacement rates,  $v_i$ . The change in  $v_i$  can be initially described by Eq 4(a) and 4(b), but near the blade leaf/locking piece link is described by Eq 5. Accordingly,  $\lambda$  is modified (Eq 1 and 2), and  $\lambda_1 = \lambda$  only if  $v_i$  is a constant. Thus, the magnitude of the change in the rate of mold pulling becomes  $Dv = v_p - v_i$ .

According to Eq 1 to 5, from the blade leaf position up to the maximum in the curve shown in Fig. 12, the rate of mold pulling should increase nonlinearly. Similarly, once the mold goes through the maximum, a nonlinear decrease is expected. The results presented thus far are valid for displacement rates of  $1.86 \times 10^{-6}$  m/s. At these low rates, the production technology of turbine blades becomes more expensive. Hence, in this work, pulling rates twice as high were employed. However, the experimental results indicated that this displacement rate is a bit too high, since it gives rise to less optimum aligned eutectics.

#### 4. Conclusions

It is possible to obtain in-situ composites of unidirectionally solidified NITAC alloys containing from 0.4 to 0.48% C. This, in turn, enables the production of turbine blade castings with aligned eutectic structures except for the edges of the locking

piece. A determination of the optimum range of carbon contents was made in the NITAC alloy. This is of considerable importance, eliminating the need for troublesome selection of the appropriate alloy chemistry to obtain eutectic structures. A flat solidification front and a fibrous eutectic microstructure were obtained in situ at displacement rates of  $1.86 \times 10^{-6}$  cm/s. The development of a plane front is self-evident, as fibers will always grow normal to the solidification front. The temperature gradient used at the solidification front was about 75 K/cm, whereas the maximum temperature of the chamber was 1650 to 1670 °C. The in-situ composite microstructures consisted of fibrous aligned TaC and a  $\gamma$ -phase matrix. In particular, it has been shown that unidirectional solidification changes the macrostructure of the blade from an equiaxed structure to a columnar one consisting of several oriented grains.

#### References

1. W. Kurz and P. Shame, Gerichtet erstarrte eutektische, *Werkstoff*, Springer-Verlag, Berlin, 1975, p 1234 (in German)
2. G. Piatti, R. Matera, and R. Pellgrini, In-Situ-Growth Composites: Growth and Morphology, *Advances in Composite Materials*, Applied Science Publishers, London, 1978, p 53
3. E. Fras, E. Guzik, and H.F. Lopez, Structure and Mechanical Properties of Unidirectionally Solidified Fe-Cr-C and Fe-Cr-X-C Alloys, *Metall. Trans. A*, Vol 19A, 1988, p 1235
4. J. Drapier, Progress in Advanced Directionally Solidified and Eutectic High Temperature Alloys, *High Temperature Alloys for Gas Turbines*, Applied Science Publishers, London, 1978, p 702
5. T. Chan, Further Assessment and Improvement of High Temperature  $\gamma$ - $\gamma'$ -NbC Composites for Advancing Turbine Blades, *Conf. In-Situ Composites III*, National Academy of Sciences, Washington, DC, 1973, p 378

6. M. McLean, Mechanical Properties of Directionally Solidified Superalloys for Gas Turbines, *High Temperature Alloys for Gas Turbines*, Applied Science Publishers, London, 1978, p 423
7. E. Thompson and F. Lemkey, Directionally Solidified Eutectic Superalloys, *Metallic-Matrix Composites*, Academic Press, New York, 1974
8. E. Fras and E. Guzik, Warunki Kierunkowej Krystalizacji Topatki Turbinowejze Stopu NITAC, *Arch. Nauki Mater.*, Vol 8, 1987, p 235 (in Polish)
9. W. Kurz and D. Fisher, Dendritic Growth in Eutectic Alloys: The Coupled Zone, *Int. Met. Rev.*, Vol 5, 1979, p 177
10. M. Burden and J. Hunt, The Extent of the Eutectic Range, *J. Cryst. Growth*, Vol 22, 1974, p 328
11. E. Thompson, Oral Discussion of Processing Eutectic Blades, *Conf. In-Situ Composites*, NMAB 308-I, National Academy of Sciences, Washington, DC, 1973, p 116
12. E. Fras and E. Guzik, Shaping of the Composite Structure in a Turbine Blade Cast in a NITAC Alloy, *Arch. Metall.*, Vol 33, 1988, p 267 (in Polish)